Light-mass yields and fine structure of mass distributions in ^{232}Th photofission

S. A. Karamian,[1] J. Adam,[1] A. G. Belov,[1] J. J. Carroll,[2] Yu. V. Norseev,[1] V. I. Stegailov,[1] and P. Chaloun[1]
[1]*Joint Institute for Nuclear Research, Dubna 141980, Russia*
[2]*Department of Physics and Astronomy, Center for Photon-Induced Processes, Youngstown State University, Youngstown, Ohio 44555*
(Received 4 November 1999; revised manuscript received 9 March 2000; published 27 June 2000)

Fission-fragment mass distributions in the ^{232}Th(γ, f) reaction have been measured from the cumulative yields of radionuclides following activation at bremsstrahlung endpoint energies $E_e = 7.5$, 12.0, and 24.0 MeV. The yields of the light nuclei ^{24}Na and ^{28}Mg were detected following activation at $E_e = 16.5$ and 24.0 MeV. Energy dependences of the symmetric mode and light nuclide yields are discussed. Fine-structure manifestations near asymmetric and symmetric masses were observed.

PACS number(s): 25.85.Jg, 25.20.−x

I. INTRODUCTION

The detection of fission fragments from their activity using radiochemistry and γ-spectroscopic methods is recognized to be the most accurate way to perform measurements of final mass distributions. In ^{232}Th(γ, f) photofission, individual mass yields were measured in Refs. [1–3] and fine-structure peaks were seen to modulate the asymmetric humps in the mass distribution. This fine structure was explained as a result of odd-even Z_f staggering in the fragment yields [2]. Near symmetry, however, the mass distribution has been studied with limited accuracy due to low reaction yields, and it has remained an open question whether fine structure also exists for the symmetric mode. The authors of Ref. [4] assumed, based on some theoretical considerations, that there would be a reduction of the odd-even staggering effect for the symmetric Z partition relative to the asymmetric one. It is reliably known that the relative intensity of mass-symmetric fission grows with an increase in the excitation energy E^* [1–3,5], and this is evidenced in a higher value of the fission barrier in ^{232}Th for the symmetric mode compared to the asymmetric mode. Clearly improved studies of fine structure near symmetric mass remain important, as well as obtaining detailed confirmation of asymmetric peak modulation.

Similarly, emission of $A \geqslant 20$ nuclei in ternary fission cannot be considered to be well understood. In the series of experiments performed by the group of Ref. [6], light charged particles from ^{1}H to ^{20}O were successfully detected with individual yields greater than 10^{-7} per fission event. Other groups [7–9] observed $A = 20 - 30$ nuclide emission in thermal-neutron-induced fission of actinide targets from ^{229}Th to ^{249}Cf. The results given in Refs. [10,11] on the detection of the ^{24}Na and ^{28}Mg radionuclides in products of ^{232}Th fission induced by charged particles and photons are, unfortunately, not very reliable. Geiger counters were used in the work of Ref. [10] and these could not differentiate between radionuclides by their radiation. Likewise, chemical separation alone is insufficient to ensure that the whole activity of fragments is completely removed from the apparent Na and Mg fractions. In addition, a background yield of ^{24}Na and ^{28}Mg nuclides may be induced in Al foils exposed to ^{4}He ions, as shown in separate measurements by the group of Ref. [12]. Such foil catchers were used in the ^{4}He ion irradiations of Th targets in [10].

The measurements of Ref. [11] were also significantly disturbed by another type of background. In Refs. [13,14] it was shown that weak γ lines present in the daughter radiation from the ^{112}Pd and ^{132}Te fragments can simulate the major γ lines of ^{24}Na and ^{28}Mg, respectively. This background was not removed in the experiment of Ref. [11] and the results were therefore unconvincing. Thus, there is considerable motivation for new experiments on the emission of light nuclei in the photofission of ^{232}Th.

In the present work, the radioactive products of ^{232}Th photofission were analyzed by their γ radiation using a high quality γ spectrometer and radiochemistry methods in order to further investigate fine structures in mass distributions and light-mass yields in the photofission of ^{232}Th.

II. MASS DISTRIBUTIONS

Historically, the existence of an asymmetric mass distribution was revealed shortly after the discovery of nuclear fission, and during many decades the asymmetric mass yields and peak-to-valley ratios were investigated. The concept of there being two independent modes of fission was formulated as early as 1951 [15], and since then, the shape and yield of the symmetric peak were also within the scope of experiments. The multimodal fission model has been discussed since the 1960s [16–18]. Now over the last decade it has become most popular to consider the assumption of Brosa *et al.* [18], that there are two asymmetric modes (standards I and II). The model of Brosa *et al.*, which additionally predicts two modes of ''cold'' fission, was used successfully to interpret many experimental results. At the same time, precision studies of the fine-structure modulation of the asymmetric mass peak [1,2,19] showed the presence of three peaks of fine structure correlated with the odd-even Z_f staggering of the yield. This is outside the predictions of standards I and II for asymmetric fission. Separately, it was shown (see the discussions in Refs. [2,19]) that the relative intensities of the fine-structure peaks depend significantly on the nucleon composition of the fissile nucleus. The details of fine structure in the mass distribution remain of interest for experimental confirmation and quantitative studies.

In Ref. [2], ^{232}Th photofission yields were measured for radioactive products whose lifetimes were longer than 1 s,

and data both on charge and mass distributions were obtained successfully from the independent post-neutron yields. In the present experiment, cumulative mass yields have been measured. Short-lived nuclides, produced from a high-intensity irradiation, create an extremely large γ radiation flux, and it is necessary to apply ''cooling'' and in some cases chemical separations before starting the γ-ray spectra measurements. After ''cooling,'' the two-coordinate (Z, N) distribution becomes projected on the mass axis by the decay of short-lived isobars. This means a loss of information on the charge distribution, but high overall sensitivity is gained in such an experimental scheme, so that it was possible to investigate some details on masses yielded at lower levels that could not be reached in the work of Ref. [2]. The present technique also made it possible to avoid uncertainties due to inaccuracies in some tabulated properties of the short-lived isotopes and due to the need for corrections to escape probabilities in the method of catcher foils. Apart from these considerations, it was simply interesting to determine whether the fine structure details of Ref. [2] could be reproduced in the another experiment carried out by a different method. This was shown to be the case.

The final fragment mass distributions have been measured at bremsstrahlung endpoint energies of 7.5, 12.0, and 24.0 MeV. The targets, made of 1 g purified thorium oxide or chloride, were irradiated with the photon flux generated by a W converter from the electron beam of the MT-25 Dubna microtron. Gamma spectra of induced activity were measured over a period of a few weeks after the irradiation, so nuclides with lifetimes ranging from hours to months were detected. For energy and efficiency calibrations, both standard sources and internal calibration methods were used. The source-to-detector distance and the lead-absorber thickness (in front of the Ge spectrometer) were varied to provide an optimum sensitivity for the γ lines of interest while conserving the best resolution (1.8 keV determined from ^{60}Co lines) and reasonable dead time ($\leqslant 20\%$) during the measurements.

The relative yields of the nuclides were determined by their γ-line counts, taking into account the quantum intensities of the γ lines, decay factors, and efficiency values. The yield of an individual mass was normally collected in the cumulative yield of the longest-lived nuclide after sequential β decays of precursive isobars. Over 50 cumulative chain yields were directly measured and from which the mass distribution was plotted. The cumulative fission products are listed in Table I with decay properties taken from the current Nuclear Data Sheets. Incomplete cumulativity and the delayed neutron effect were taken into account, although the corresponding corrections typically did not exceed 10% of the measured yield. The absolute calibration of the mass-distribution curve was based on a normalization to a 200% value for the integral yield of all masses. For the reconstruction of the mass distributions, neither any recalculation of the final to the initial masses nor any reflection of the points to the complementary masses was performed since any simulation of the effect of prompt neutron emission could have introduced additional uncertainty.

The final fragment mass distributions are given in Fig. 1 as they appear from the cumulative yields of radionuclides. Being plotted in a logarithmic scale, they show clearly that the symmetric mode probability strongly increases with the growth in photon endpoint energy. The fine details of mass distributions near the maxima, however, are more clearly seen in Fig. 2 where the same mass distributions are plotted on a linear scale. In agreement with Ref. [2], narrow peaks at mass numbers $A_f = 134$, 140, 144 and at the complementary mass values are observed. These fine structures can be attributed to odd-even Z_f staggering of the fragment yield. Figure 2 shows that the amplitude of staggering decreases with the growth of the excitation energy because of pairing destruction, also in agreement with the results of Ref. [2]. Despite quite different methods, the existence of fine-structure peaks was reproduced. The stability of these features in the various experiments is important, meaning that their origin is inherent in the fundamental fission process, not in any secondary processes or in the detection scheme.

The integral yield ratio of the symmetric to asymmetric modes was deduced using the bimodal decomposition procedure. The total yield of the symmetric (asymmetric) peak was calculated as a sum of individual mass yields using the interpolation and peak decomposition procedures. The Gaussian fit was not applied since the shape of asymmetric peak is not well described by a Gaussian. The results are compared with the literature data in Fig. 3; different reactions are reduced to the mean excitation energy of the compound nucleus for comparison. The points in Fig. 3 belong mostly to the bremsstrahlung-induced fission; thus, the corresponding E_e values for the points are also given according to the upper horizontal axis scale. The present measurements are in reasonable agreement with other data taken for thorium fission induced by photons [1,5] and neutrons [20,21]. Only the ^{232}Th(p, f) reaction shows a somewhat higher relative yield of the symmetric mode [22].

The accuracy of the present measurements was sufficient to search for a manifestation of fine structure at the symmetric mode maximum, at least in the case of $E_e = 24$ MeV where the probability of this mode approaches about 6%. Enhanced yields were found for $A = 112$ and 113 masses. To understand the origin of this enhancement, one must consider the possibility that it reflects a double yield for products of the absolutely symmetric partition: $A_f = A_c/2$ (where A_c is an even number). Such a delta-function peak can be expected to be shifted and smoothed due to prompt-neutron emission, but a lower amplitude relic can survive. The final mass numbers $A_f = 113$ for both fragments correspond to the neutron multiplicity $\nu = 6$ and consequently to an excitation energy of the fragments of about 40 MeV ($\overline{B_n} \approx 5.5$ MeV). Such an excitation energy can be expected to be released in the symmetric fission of the ^{232}Th nucleus at the initial mean excitation of 14 MeV (corresponding to $E_e = 24$ MeV).

The symmetry of scission figure (Fig. 4) suggests an explanation for the presence or absence of the delta-function peak at the center of the mass distribution. Consider the axially symmetric figure with an elongated neck as the standard scission configuration. Each individual mass number of a fragment (and its complementary one) corresponds to a well-defined position of a rupture plane in the neck. When the figure possesses reflection symmetry, the left and right locations of the corresponding rupture planes are identical and

TABLE I. Decay properties of nuclides accumulating the isobaric chain yields in fission. The designation D indicates a γ line emitted by decay of the daughter nucleus. When lifetimes of precursor and daughter are comparable, both $T_{1/2}$ are given.

Nuclide	$T_{1/2}$	E_γ [keV]	I_γ [%]	Nuclide	$T_{1/2}$	E_γ [keV]	I_γ [%]
^{72}Zn→^{72}Ga	46.5 h→14.1 h	2202	27.1	^{117}Cd	2.49 h	1303	18.4
^{73}Ga	4.86 h	297	80	^{117m}Cd	3.36 h	1997	26.2
^{75}Ge	1.38 h	265	11.3	^{125}Sb	2.73 y	428	29.4
^{77}Ge	11.3 h	714	6.8	^{127}Sb	3.85 d	686	35.3
^{78}Ge→^{78}As	1.47 h→1.51 h	277, 614	96, 54	^{128}Sn	0.99 h	482	58
^{83}Se	0.37 h	357	68.6	^{129}Sb	4.4 h	813, 915	43.5, 20.3
^{84}Br	0.53 h	1898	14.5	^{131}I	8.02 d	637	7.3
^{85m}Kr	4.48 h	151, 305	75, 14	^{132}Te→^{132}I	3.20 d→2.3 h	668	100
^{87}Kr	1.27 h	403, 2555	50, 9.2	^{133}I	20.8 h	530	87
^{88}Kr→^{88}Rb	2.84 h→0.3 h	1836, 2392	22, 35	^{134}Te	0.7 h	767	29
^{89}Rb	0.25 h	1032, 1248	64, 47	^{134}I	0.867 h	847, 884	95.4, 65.9
^{91}Sr	9.63 h	750, 1024	24, 33	^{135}I	6.61 h	1678	9.52
^{92}Sr	2.71 h	953, 1384	3.6, 90	^{138}Cs	0.56 h	1436	76.3
^{92}Y	3.54 h	934	13.9	^{139}Ba	1.38 h	166	23.8
^{93}Y	10.1 h	1918	1.4	^{140}Ba →^{140}La	12.75 d →40.2 h	537, 1596	24, 96
^{94}Y	0.31 h	919	56				
^{95}Zr	64.03 d	757	55.4	^{141}La	3.92 h	1355	1.64
^{97}Zr	17.0 h	658 (D)	100	^{142}La	1.52 h	1901, 2398	7.2, 13.3
^{99}Mo	2.75 d	740	12.1	^{143}Ce	33 h	293, 722	43, 5.33
^{103}Ru	39.3 d	497	89.5	^{144}Ce	285 d	134, 697 (D)	11.1, 1.34
^{105}Ru	4.44 h	469	17.3	^{145}Pr	5.98 h	676	0.51
^{105}Rh	35.4 h	319	19	^{146}Pr	0.4 h	1525	16
^{106}Ru	373.6 d	622 (D)	9.8	^{147}Nd	10.98 d	531	13
^{111}Ag	7.45 d	342	6.7	^{149}Nd	1.73 h	211, 270	26, 11
^{112}Pd →^{112}Ag	21.1 h→3.12 h	617, 1388	43.5, 5.4	^{149}Pm	2.21 d	286	3.1
				^{151}Pm	28.4 h	340	22.4
^{113}Ag	5.37 h	299	10.6	^{156}Eu	15.2 d	812, 1231	9.8, 8.0
^{115}Cd	2.23 d	336	46				

both lead to the same mass asymmetry of the fragments. In this case, the $A_f = A_c/2$ yield is not exceptionally high, with other partitions also having doubled yields because of two possibilities for rupture plane locations. Another situation takes place when there is reflection asymmetry of the scission figure. Only one rupture plane corresponds to any pair of fragments, so all products have a single yield, except the $A_f = A_c/2$ yield which is doubled because this is a pair of identical mass numbers. Thus, any observation of a fine-structure peak at the center of the fragment mass distribution indicates the reflection asymmetry of the scission figure.

III. LIGHT NUCLIDE YIELDS

To search for yields of such light nuclides as ^{7}Be, ^{24}Na, ^{28}Mg, ^{38}S, and ^{59}Fe in photon-induced fission, purified $ThCl_4$ targets were irradiated by bremsstrahlung with $E_e = 12$, 16.5, and 24 MeV. The decay properties of radionuclides sought in the measurements are listed in Table II, as given in Nuclear Data Sheets. The ^{24}Na and ^{28}Mg nuclides have half-lives of 15 and 21 h and abundant high-energy γ lines of 2753.9 keV and 1778.8 keV, respectively. These properties enabled them to be identified with high sensitivity. The radionuclides ^{7}Be, ^{38}S, and ^{59}Fe do not have such convenient decay properties, and so only upper limits for their yields could be deduced. The following describes the detection of ^{24}Na and ^{28}Mg radionuclides in the products of ^{232}Th photofission.

The purity of the target was verified by the absence, after irradiation, of such typical products of photonuclear reactions as ^{22}Na, ^{51}Cr, ^{54}Mn, ^{58}Co, and ^{65}Zn. Radiochemical isolation of the fraction of alkali and alkali-earth metals was performed after 4 h ''cooling'' of the target, which was necessary for the decay of a high activity of short-lived fission products. Then γ spectroscopic measurements were performed using an absorber composed of 10–20 mm Pb and 1 mm each Cd and Cu plates. The transmission coefficient was nearly 30–60 % for the high-energy γ quanta of ^{28}Mg and ^{24}Na, while γ quanta with $E_\gamma < 500$ keV were absorbed. The energy resolution and calibration were not degraded signifi-

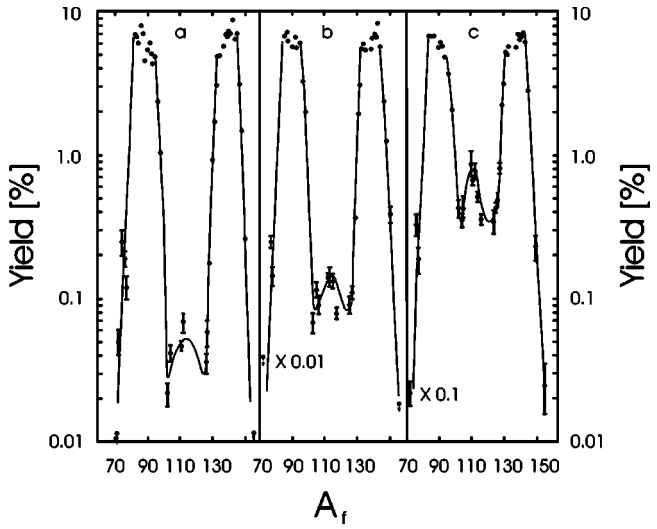

FIG. 1. Final fragment mass distributions measured for ^{232}Th photofission at (a) $E_e = 7.5$ MeV, (b) 12.0 MeV, and (c) 24.0 MeV. Solid curves are given to guide the eye to the experimental points.

cantly even at a count rate of about 20 000 Hz, when the dead time reached 20% of the real time. The source contained Sr, Ba, Ra, and other radionuclides and gamma lines of ^{140}Ba, ^{228}Ra, and ^{224}Ra were used for internal calibration of the spectrometer. Lines from ^{91}Sr and ^{140}Ba were used to normalize the yield per fission event. As an example, Fig. 5 shows a full γ-ray spectrum taken with a 17 mm Pb absorber.

The chemically isolated fraction was specially purified to remove any radioactive fragments of Pd and Te. This was necessary since weak γ lines from the decay chains ^{112}Pd $\rightarrow ^{112}$Ag$\rightarrow ^{112}$Cd (γ 2752.8 keV) and ^{132}Te$\rightarrow ^{132}$I $\rightarrow ^{132}$Xe (γ 1778.6 keV) could have simulated the yield of ^{24}Na and ^{28}Mg, respectively, on a level of 10^{-5} per fission. After chemical purification, the remaining background was calibrated by the most intense lines of the nuclides in Table II and subtracted. Having done so, ^{24}Na and ^{28}Mg radionuclides could be detected with yields below 10^{-6} per fission event at $E_e = 16.5$ and 24 MeV. The relevant sections of a

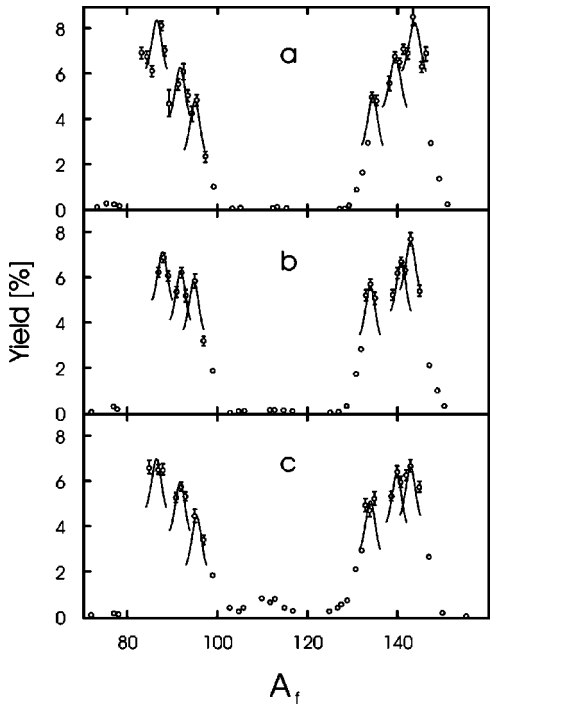

FIG. 2. Data of Fig. 1 plotted on a linear scale. Solid curves are given to guide the eye to the experimental points.

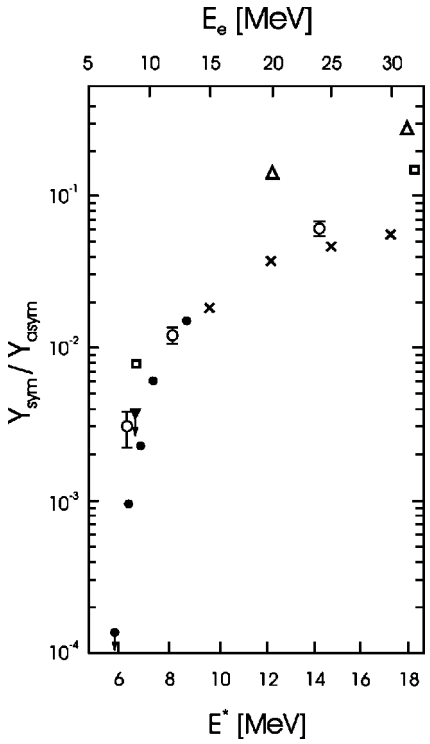

FIG. 3. Symmetric-to-asymmetric yield ratio as a function of E^* and E_e from (closed circles) Ref. [1], (crosses) Ref. [5], (open circles) present results, (open squares) Ref. [20], (inverted triangles) Ref. [21], and (triangles) Ref. [22]. The data correspond to ^{232}Th(γ, f) reactions from Refs. [1,5] and the present work, ^{232}Th(n, f) from Ref. [20], ^{229}Th(n_{th}, f) from Ref. [21], and ^{232}Th(p, f) from Ref. [22].

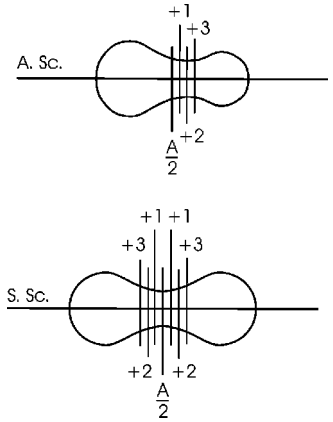

FIG. 4. Illustration of the scission for the different reflection symmetry cases. The rupture planes corresponding to fragment masses of $(0.5A_c + n)$, $n = 0$, 1, 2, and 3, are shown schematically.

TABLE II. Gamma lines used in measurements of the light nuclide yields.

Nuclide	$T_{1/2}$	E_γ [keV]	I_γ [%]
^{7}Be	53.3 d	477.6	10.4
^{24}Na	15.0 h	1368.5	100
		2753.9	100
^{28}Mg→^{28}Al	20.9 h →2.2 min	1342.2	54.0
		1778.8	100
^{38}S→^{38}Cl	2.84 h→37 min	1941.9	84.0
		2167.6	42.4
^{59}Fe	44.5 d	1099.3	56.5
		1291.6	43.2
^{91}Sr→^{91m}Y	9.6 h →49 min	555.6	61.3
^{112}Pd →^{112}Ag	21.1 h →3.1 h	617.4	43.5
		2752.8	0.11
^{132}Te →^{132}I	76.3 h →2.3 h	667.7	100
		1778.6	0.08
^{140}Ba →^{140}La	12.75 d→40.3 h	537.3	24.4
		1596.2	95.4

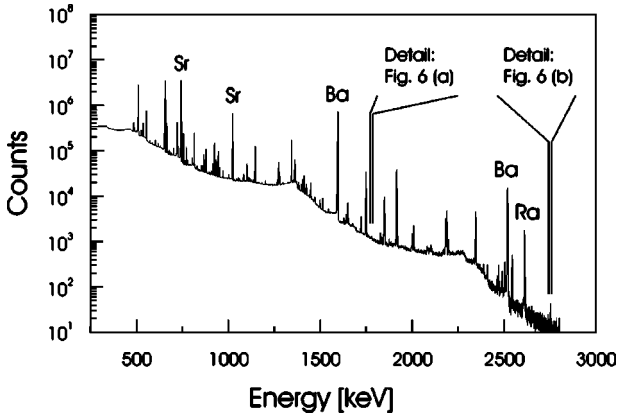

FIG. 5. Complete energy range γ-ray spectrum of ^{232}Th photofission products at $E_e=24$ MeV. The spectrum was taken with a 17-mm Pb filter inserted in front of the Ge detector. The indicated intense lines correspond to the alkali-earth metal radionuclides ^{91}Sr, ^{140}Ba→^{140}La, and ^{224}Ra. The latter radionuclide, being a precursor of ^{208}Tl, is present in the target as a daughter product of ^{232}Th decay, and the fission fragment ^{140}Ba is a precursor of the shorter-lived ^{140}La emitting the marked lines.

typical γ spectrum, taken at $E_e=24$ MeV, are shown in Fig. 6. The statistics accumulated at $E_e=16.5$ MeV were worse, although the lines of ^{28}Mg and ^{24}Na were still observed clearly and their decays agreed with the tabulated half-lives. The sensitivity of the measurements decreased as the endpoint energy was reduced because of the overall reduction of bremsstrahlung flux. The upper limits of the ^{24}Na and ^{28}Mg yields were only estimated at $E_e=12$ MeV. The results are given in Table III.

Yields of ^{24}Na and ^{28}Mg, being about 10^{-6} per fission, are consistent with previous results [13]. There upper limits were established to be $\leqslant(1-2)\times10^{-7}$ per (γ,n) reaction event, and the well-known ratio of fission to photoneutron reaction yields is about 0.1 for ^{232}Th. The present, smaller, upper limit for the ^{59}Fe yield is in agreement with the result of the Munich group [23], which observed an absence of ^{60}Fe in products of thermal-neutron-induced ^{235}U fission. The present yield estimates for ^{7}Be and ^{38}S have no physical significance because the sensitivity was limited by backgrounds.

The mechanism for third-fragment emission from an elongated fissile nucleus does not imply a strong energy dependence of the yield since the Coulomb barrier penetration factor is insignificant in this case. Third fragment emission is regulated by the formation and partition probabilities at the scission point, when the barrier has already been overcome. A steep energy dependence in this case should be replaced by a weaker one originating from the deficit of free energy for third-fragment formation. Experimentally, the probability of long-range α particle emission [20], shown in Fig. 7(a), indeed demonstrates a surprising stability over a wide range of excitation energies. The present results do not show such a strong dependence of the light nuclide yields on the compound nucleus excitation as was reported in Ref. [10]. The yield is decreased by a factor 0.5 when the mean E^* is reduced from 14 to 11 MeV; in fact, at 8 MeV no yield above the sensitivity limit could be detected, although that limit was not particularly restrictive. The present results support the conclusion that emission from scission configuration is the preferable mechanism not only for α particles, but also for nuclei as massive as $A=24$ and 28. The present results on ^{24}Na and ^{28}Mg are compared in Fig. 7(b) with the yields reported in Refs. [10,11] and are not in good agreement. This can be explained, as discussed above, by considering the less effective nature of the methods used in [10,11]. This disagreement requires, nevertheless, some additional comments

TABLE III. Experimental results for light nuclide yield estimates from the ^{232}Th(γ,f) reaction at three values of bremsstrahlung endpoint energy.

Reaction product	Yield per fission event 24 MeV	16.5 MeV	12 MeV
^{7}Be	$\leqslant1.1\times10^{-4}$	–	$\leqslant1.0\times10^{-4}$
^{24}Na	$(1.0\pm0.2)\times10^{-6}$	$(0.33\pm0.10)\times10^{-6}$	$\leqslant0.5\times10^{-6}$
^{28}Mg	$(0.85\pm0.15)\times10^{-6}$	$(0.46\pm0.15)\times10^{-6}$	$\leqslant1.2\times10^{-6}$
^{38}S	$\leqslant2.5\times10^{-5}$	–	$\leqslant1.0\times10^{-6}$
^{59}Fe	$\leqslant1.0\times10^{-7}$	–	$\leqslant2.6\times10^{-6}$

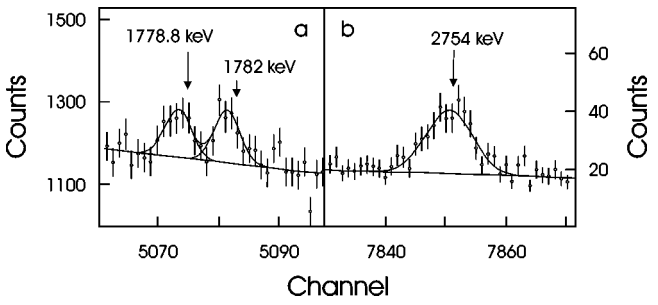

FIG. 6. Sections of γ-ray spectra showing signatures of (a) ^{28}Mg and (b) ^{24}Na in the experiment on ^{232}Th fission at $E_e = 24$ MeV.

to specify and distinguish the conditions of the experiments which are being compared. Background production of ^{24}Na and ^{28}Mg in Al catchers is really characterized by a strong energy dependence [12] and this background can be higher than the yield of products in Th fission. Also, it is well known that the nonselective method of activity detection using Geiger counters required an extremely high degree of chemical purification. In such an experiment, the efficiency of chemical isolation can be easily decreased or even reduced essentially to zero and this would strongly influence the results to suggest a too-small yield. These two reasons may explain both the lower yields and stronger energy dependences given in Ref. [10] as compared to the present results.

A characterization of the yield energy dependence is important to clarify the mechanism of light nuclei emission. For the case of bremsstrahlung induced reactions (the present experiment and that of Ref. [11]), the E^* distribution of fissile compound nuclei can be calculated using the incident

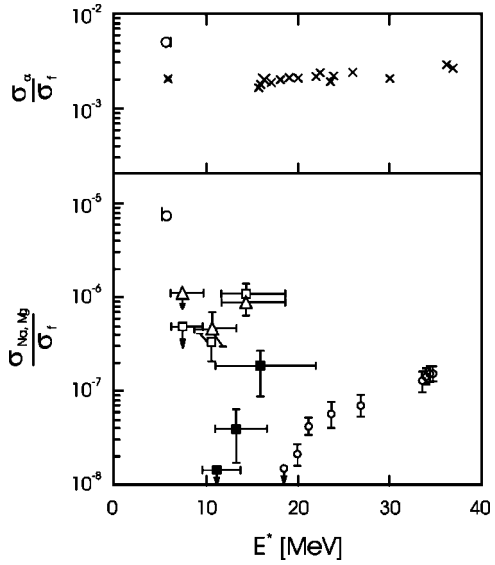

FIG. 7. Excitation functions for the relative ternary fission probability. Panels show (a) long-range α particle emission in the case of uranium fission induced by neutrons and ^{4}He ions [20] and (b) ^{24}Na and ^{28}Mg radionuclide yields from Refs. [10,11], as given by open circles and solid squares, respectively, and from the present experiment open squares for ^{24}Na and open triangles for ^{28}Mg.

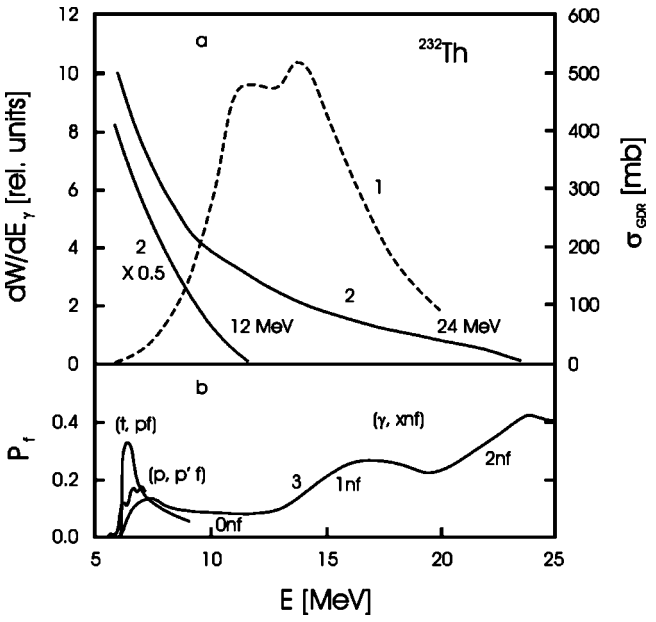

FIG. 8. Excitation functions for the cross section of photon absorption by ^{232}Th nuclei [24] (dashed curve 1 plotted by the right-hand axis), and for fission probability [25,26] (curve 3). Calculated bremsstrahlung spectra are also shown by curve 2.

radiation spectrum in combination with the photon-absorption and fission-probability excitation functions. In Fig. 8, the calculated bremsstrahlung spectrum and two other functions, deduced from Refs. [24–26] for ^{232}Th, are shown. The giant dipole resonance (photon-absorption) cross section was taken in accordance with [24], and the probability of (γ, xnf) fission events was calculated from those values known for (n, xnf) reactions [25]. Reference [26] and citations therein define this probability function $P_f(E^*)$ near the ^{232}Th fission barrier at $B_f = 6.0$ MeV. The E^* distribution of fissile compound nuclei was evaluated as a product of curves 1, 2, and 3 shown in Fig. 8. Finally, mean E^* and half-width values were found. These define the horizontal positions and error bars for the data of Fig. 7(b), corresponding both to the present measurements and to those of Ref. [11]. This is the only correct presentation possible for data taken with a continuous bremsstrahlung spectrum. The discrepancy is, nevertheless, evident between the three sets of data shown in Fig. 6(b).

The present values of the yield look too high in Fig. 7(b) in comparison with Refs. [10,11]. They are, however, compatible with other data. The present results are in agreement with the trend established in Ref. [6] and extrapolated to higher masses of third fragments using calculations of Ref. [7] based on the Halpern model of ternary fission [27]. As measured in Ref. [7], the yield of the ^{24}Ne nucleus is greater than 2×10^{-7} per fission event for all heavy targets, from ^{239}Pu up to ^{249}Cf, and ^{27}Na has an approximately 50% lower yield. In our case of the ^{232}Th(γ, f) reaction, the mean excitation energy of the compound nucleus is higher by 6 – 8 MeV than for the (n_{th}, f) reactions employed in the work of Ref. [7]. Even higher energies are present because of the wide E^* distribution mentioned above. Thus, the total re-

lease of energy in ^{232}Th(γ, f) reactions can be comparable with that from ^{239}Pu(n_{th}, f) reactions. In addition, cumulative yields of the $A=24$ and 28 isobaric chains were detected here, while the experimental method used in Refs. [6–9] was based on the detection of the prompt products emitted with definite kinetic energy and charge state and selected by a kinematical separator and ionization chamber. In that instance the individual yields must be integrated over the entire energy spectrum, all charge states and nuclear charges in order to make a comparison with the total yield of specific A isobars. In such a context, the yields below 10^{-6} per fission event for $A=24$ and 28 masses measured in the present work do not strongly contradict to the series of experiments carried out with thermal neutrons [6–9].

The yields measured here are perhaps slightly higher than could have been expected from the experiments cited above. One more factor may contribute to this. The authors of Ref. [28] proposed a new mechanism of ternary fission in which a mass fragment of intermediate mass remains almost static, unaccelerated by the Coulomb field since it is placed on the axis between the two massive fragments at scission. This mechanism seems somewhat exotic, but in some special conditions it can, obviously, provide a significant contribution to the yield of ternary fission. The total kinetic energy of the three fragments is lower in this case with respect to the variant when all three fragments are accelerated. Because of the gain in free energy, a measurable contribution to the total yield of these rare ternary fission products can be expected. For long-range α particles, it is probably unimportant since there is not a significant deficit of free energy. Products of low kinetic energy were detected successfully in the activation – radiochemistry – γ-spectroscopy method applied in the present work. Thus, the total actual yield may indeed be larger than that detected by the kinematical separator method. This point should be studied in additional experiments.

In general, the magnitude of yield from these reactions merits future studies. For example, in the well-known book *The Nuclear Fission Process*, edited by Wagemans, the probability of ''true'' ternary fission is discussed in a separate paragraph [29]. Large-scale scatter is apparent between yields deduced from different experiments. It is important to note that the value of about 10^{-6} per fission for $A=20-30$ products found here is near the center of gravity of the scattered values referenced in that tome. Thus, the present results are consistent with the analysis of Ref. [29]. The probability for true ternary fission is significantly increased when fission is induced by heavy ions. This interesting phenomenon was detected in the experiments of Refs. [30,31] and explained by an original model assuming the sequential, two-step fission (cascade fission) of systems heavier than ^{40}Ar+^{238}U. It is difficult to compare the results of heavy-ion-induced fission with photon or α-induced fission because new mechanisms can participate, in addition to there being a large difference in Z^2/A and angular momenta values.

A group of inconsistent results was reported in Refs. [10,23,32–38] on the yields of fission products with masses of $30<A<70$ and $A>170$. From the present measurements, an upper limit of less than 10^{-7} per fission was deduced for the yield of $A=59$ nuclei at the bremsstrahlung endpoint energy of 24 MeV. Within an order of magnitude, this value is in accordance with the results of Refs. [23,33,36,37] which is quite good considering the different reactions and excitation energies.

IV. SUMMARY

Final fragment mass distributions were measured in the ^{232}Th(γ, f) reaction at mean excitation energies of 6.5, 8.0, and 14.0 MeV using cumulative isobaric yields. The relative probability of the symmetric mode and the fine-structure amplitudes were found to be in accordance with the results of previous publications. The stability of the observed fine peculiarities despite variation of experimental methods confirms their inherent nature, coming from the formation process of the fragments. The presence of a fine-structure peak near the symmetric mode maximum is tested and the mechanism is discussed. The yields of ^{24}Na and ^{28}Mg radionuclides are reliably detected and the emission of light nuclei is evaluated within some new suggestions to clarify the mechanism of ternary fission.

[1] M. Piessens, E. Jacobs, S. Pommé, and D. De Frenne, Nucl. Phys. **A556**, 88 (1993).

[2] K. Persyn, E. Jacobs, S. Pommé, K. Govaert, and M. Yoneama, Nucl. Phys. **A620**, 171 (1997).

[3] J. C. Hogan, A. E. Richardson, J. L. Meason, and H. L. Wright, Phys. Rev. C **16**, 2296 (1977).

[4] M. de Jong, C. Böckstiegel, H.-G. Clerc, A. Grewe, A. Junghans, J. Müller, J. Benlliure, A. Heinz, K.-H. Schmidt, M. Pfützner, A. Ignatyuk, and G. Kudyaev, Nucl. Phys. **A616**, 363 (1997).

[5] W. Günther, K. Huber, U. Kneißl, H. Krieger, and H. J. Maier, Z. Phys. A **295**, 333 (1980).

[6] A. A. Vorobiev, D. M. Seliverstov, V. T. Grachov, I. A. Kondurov, A. M. Nikitin, N. N. Smirnov, and Yu. K. Zalite, Phys. Lett. **40B**, 102 (1972).

[7] N. Wöstheinrich, R. Pfrister, F. Gönnenwein, H. O. Denschlag, H. Faust, and S. Oberstedt, in *Proceedings of the 4th International Workshop on Dynamical Aspects of Nuclear Fission*, Častá-Papiernička, Slovakia, 1998, edited by Yu. Ts. Oganessian, J. Kliman, and S. Gmuca (World Scientific, Singapore, 1999), p. 189.

[8] U. Köster, H. Faust, G. Fioni, T. Friedrichs, M. Groß, and S. Oberstedt, Beschleunigerlaboratorium Jahresbericht 1998, Technische Universität München (unpublished), p. 8.

[9] F. Gönnenwein, in Proceedings of the 2nd International Workshop On Dynamical Aspects of Nuclear Fission, JINR, Dubna, Russia, 1994, Report No. E7-94-19, p. 47.

[10] T. C. Roginski, M. E. Davies, and J. W. Cobble, Phys. Rev. C **4**, 1361 (1971); R. H. Iyer and J. W. Cobble, Phys. Rev. **172**, 1186 (1968).

[11] Yu. P. Gangrsky, Ch. G. Christov, and V. M. Vasko, Yad. Fiz.

44, 294 (1986) [Sov. J. Nucl. Phys. **44**, 184 (1986)].
[12] S. A. Karamian, J. Adam, A. G. Belov, Yu. V. Norseev, V. I. Stegailov, and P. Chaloun, Yad. Fiz. **63**, 787 (2000) [Phys. At. Nucl. **63**, 718 (2000)]; S. A Karamian, J. Adam, V. I. Stegailov, and P. Chaloun, in *Abstracts of the 47th Annual Conference on Nuclear Spectroscopy and Nuclear Structure* (Nauka, St. Petersburg, 1997), p. 322.
[13] S. A. Karamian, J. Adam, A. G. Belov, P. Chaloun, Yu. V. Norseev, and V. I. Stegailov, in *Proceedings of the International Workshop on Research with Fission Fragments*, edited by T. von Egidy, F. J. Hartmann, D. Habs, K. E. G. Löbner, and H. Nifenecker (World Scientific, Singapore, 1997), p. 199.
[14] S. A. Karamian, J. Adam, A. G. Belov, Yu. V. Norseev, and P. Chaloun, Izv. Acad. Nauk, Ser. Fiz. **61**, 2233 (1997).
[15] A. Turkevich and J. B. Niday, Phys. Rev. **84**, 52 (1951).
[16] H. Faissner and K. Wildermuth, Nucl. Phys. **58**, 177 (1964).
[17] A. Sandulescu, D. N. Poenaru, and W. Greiner, Part. Nuclei **11**, 1334 (1980).
[18] U. Brosa, S. Grossmann, and A. Müller, Phys. Rep. **197**, 167 (1990).
[19] C. Wagemans, P. Schillebeeckx, and A. Deruytter, Nucl. Phys. **A502**, 287c (1989).
[20] V. M. Gorbachev, Yu. S. Zamiatnin, and A. A. Lbov, *Interaction of Radiation with Heavy Nuclei and Fission* (Atomizdat, Moscow, 1976).
[21] N. Boucheneb, P. Geltenbort, M. Asghar, G. Barreau, T. P. Doan, F. Gönnenwein, B. Leroux, A. Oed, and A. Sicre, Nucl. Phys. **A502**, 261c (1989).
[22] S. V. Zhdanov, M. G. Itkis, S. I. Mulgin, V. N. Okolovich, A. Ya. Rusanov, G. N. Smirenkin, and M. I. Subbotin, Yad. Fiz. **55**, 3169 (1992) [Sov. J. Nucl. Phys. **55**, 1766 (1992)].
[23] G. Korschinek, T. Faestermann, K. Knie, and C. Schmidt, Radiocarbon **38**, 68 (1996); A. Elhart, T. Faestermann, K. Knie, G. Korschinek, G. Rugel, C. Lierse, and A. Stippschild, Berschleunigerlaboratorium Jahresbericht 1997, Technische Universität München (unpublished), p. 49.
[24] S. S. Dietrich and B. L. Berman, At. Data Nucl. Data Tables **38**, 199 (1988).
[25] V. McLane, Ch. L. Dunford, and R. F. Rose, *Neutron Cross Sections* (Academic, New York, 1988), Vol 2.
[26] G. N. Smirenkin and A. S. Soldatov, Yad. Fiz. **59**, 203 (1996) [Phys. At. Nucl. **59**, 185 (1996)].
[27] I. Halpern, Annu. Rev. Nucl. Sci. **21**, 245 (1971).
[28] G. F. Solyakin and A. V. Kravtsov, Phys. Rev. C **54**, 1798 (1996).
[29] C. Wagemans, in *The Nuclear Fission Process*, edited by C. Wagemans (CRC, Boca Raton, 1991), p. 574.
[30] R. L. Fleischer, P. B. Price, R. M. Walker, and E. K. Hubbard, Phys. Rev. **143**, 943 (1966).
[31] S. A. Karamian, I. V. Kusnetsov, Yu. Ts. Oganessian, and Yu. E. Penionzhkevich, Yad. Fiz. **5**, 959 (1967) [Sov. J. Nucl. Phys. **5**, 684 (1966)].
[32] M. L. Muga and C. R. Rice, in *Proceedings of the Symposium on the Physics and Chemistry of Fission* (IAEA, Vienna, 1969), p. 707.
[33] R. H. Stoener and M. Hillman, Phys. Rev. **142**, 716 (1966).
[34] R. H. Iyer, V. K. Bhargava, V. K. Rao, S. G. Marathe, and S. M. Sahakundu, in *Proceedings of the Symposium on the Physics and Chemistry of Fission* (IAEA, Vienna, 1980), Vol 2, p. 311.
[35] G. Barreau, A. Sicre, F. Caïtucoli, M. Asghar, T. P. Doan, B. Leroux, G. Martinez, and T. Benfoughal, Nucl. Phys. **A432**, 411 (1985).
[36] P. Shall, P. Heeg, M. Mutterer, and J. P. Theobald, Phys. Lett. B **191**, 339 (1987).
[37] V. Grachov, Y. Gusev, I. Kondurov, A. Nikitin, D. Seliverstov, N. Smirnov, A. Vorobiev, and Y. Zalite, Leningrad Nuclear Physics Institute Research Report 1986 (unpublished), p. 78.
[38] D. G. Sarantites, D. R. Bowman, G. J. Wozniak, R. J. Charity, Z. H. Liu, R. J. McDonald, M. A. McMahan, and L. G. Moretto, Phys. Lett. B **218**, 427 (1989).